Basic radiation from an off-centered dipole

Jérôme Pétri

Observatoire astronomique de Strasbourg, Université de Strasbourg, France.

PNS, July 2017, Saint-Petersburg

Summary

The academic problem

Rotate a magnetic dipole in vacuum.
Assume for simplicity

1) a perfect sphere.
2) a perfect conductor.

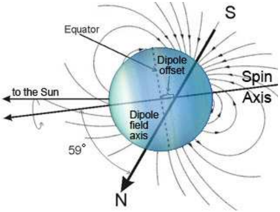

Example of offset dipole (for Uranus).

Where to put the magnetic moment w.r.T the centre of the sphere?

a) if both coincide ⇒ (Deutsch, 1955).
b) if they are offset ⇒ (Pétri, 2015, 2016).

Observational signature through phase-resolved polarisation:

a) ⇒ rotating vector model (RVM) (Radhakrishnan & Cooke, 1969).
b) ⇒ decentred RVM (DRVM) (Pétri, 2017).

and multiwavelength light-curve fitting.

Method of solution for the electromagnetic field

- looking for stationary solutions rotating at a solid body rotation rate Ω.
- any stationary electromagnetic field in vacuum can be expanded into a series of multipoles with order (ℓ, m).

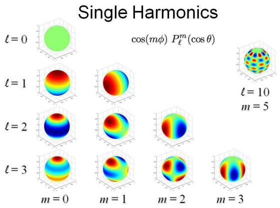

- weights are computed according to the RADIAL magnetic field B^r at the surface R.

Any exact solution to Maxwell equations is a linear superposition of single multiple solutions (weights are given by $B^r(R)$ at the stellar surface).

Exact multipolar expansion of electromagnetic fields

Any time harmonic solution at frequency Ω in vacuum can be cast into an exact divergencelessness form (Pétri, 2015)

$$\mathbf{D}(r,\vartheta,\varphi,t) = \sum_{\ell=1}^{\infty} \nabla \times [a^{\rm D}_{\ell,0} \, \frac{\mathbf{\Phi}_{\ell,0}}{r^{\ell+1}}] + \sum_{\ell=1}^{\infty} \sum_{m=-\ell, m\neq 0}^{\ell}$$

$$\left(\nabla \times [a^{\rm D}_{\ell,m} \, h_\ell^{(1)}(k_m \, r) \, \mathbf{\Phi}_{\ell,m}] + i \, \varepsilon_0 \, m \, \Omega \, a^{\rm B}_{\ell,m} \, h_\ell^{(1)}(k_m \, r) \, \mathbf{\Phi}_{\ell,m} \right) \, e^{-i \, m \, \Omega \, t}$$

$$\mathbf{B}(r,\vartheta,\varphi,t) = \sum_{\ell=1}^{\infty} \nabla \times [a^{\rm B}_{\ell,0} \, \frac{\mathbf{\Phi}_{\ell,0}}{r^{\ell+1}}] + \sum_{\ell=1}^{\infty} \sum_{m=-\ell, m\neq 0}^{\ell}$$

$$\left(\nabla \times [a^{\rm B}_{\ell,m} \, h_\ell^{(1)}(k_m \, r) \, \mathbf{\Phi}_{\ell,m}] - i \, \mu_0 \, m \, \Omega \, a^{\rm D}_{\ell,m} \, h_\ell^{(1)}(k_m \, r) \, \mathbf{\Phi}_{\ell,m} \right) \, e^{-i \, m \, \Omega \, t}$$

- $\mathbf{\Phi}_{\ell,m}$ vector spherical harmonics.
- $\{a^{\rm D}_{\ell,m}, a^{\rm B}_{\ell,m}\}$ constants depending on boundary conditions at stellar surface.
- $h_\ell^{(1)}(k_m \, r)$ are spherical Hankel functions of first kind with $k_m = m \, k$.

$\Rightarrow$ only outgoing wave solutions retained.

How to compute the constants of integration $\{a^{\rm D}_{\ell,m}, a^{\rm B}_{\ell,m}\}$?

Constants of integration for magnetic part

- Exact vacuum solutions for rotating fields require only radial magnetic field component B^r at surface (Pétri, 2015).

⇒ expand it into spherical harmonics

$$B^r(R) = \sum_{\ell,m} - \frac{\sqrt{\ell\,(\ell+1)}}{R} \, f^{\mathrm{B}}_{\ell,m}(R) \, Y_{\ell,m}(\vartheta,\varphi)$$

- Solutions for rotating multipoles follow immediately.
- Constants are given for asymmetric modes $m > 0$ by

$$a^{\mathrm{B}}_{\ell,m} = \frac{f^{\mathrm{B}}_{\ell,m}(R)}{h^{(1)}_{\ell}(k_m\,R)}$$

- and for the axisymmetric case $m = 0$ by

$$a^{\mathrm{B}}_{\ell,0} = R^{\ell+1} \, f^{\mathrm{B}}_{\ell,0}(R).$$

Constants of integration for electric part

- the non-vanishing electric field coefficients $a^{\mathrm{D}}_{\ell,m}$ for asymmetric mode $m > 0$

$$a^{\mathrm{D}}_{\ell+1,m} \; \partial_r (r \, h^{(1)}_{\ell+1}(k_m \, r)) \Big|_{r=R} = \varepsilon_0 \, R \, \Omega \, \sqrt{\ell \, (\ell+2)} \, J_{\ell+1,m} \, f^{\mathrm{B}}_{\ell,m}(R)$$

$$a^{\mathrm{D}}_{\ell-1,m} \; \partial_r (r \, h^{(1)}_{\ell-1}(k_m \, r)) \Big|_{r=R} = -\varepsilon_0 \, R \, \Omega \, \sqrt{(\ell-1) \, (\ell+1)} \, J_{\ell,m} \, f^{\mathrm{B}}_{\ell,m}(R)$$

where the constants $J_{\ell,m} = \sqrt{\frac{\ell^2 - m^2}{4 \, \ell^2 - 1}}$.

- For axisymmetric mode $m = 0$

$$(\ell+1) \, a^{\mathrm{D}}_{\ell+1,0} = -\varepsilon_0 \, R^{\ell+3} \, \Omega \, \sqrt{\ell \, (\ell+2)} \, J_{\ell+1,0} \, f^{\mathrm{B}}_{\ell,0}(R)$$

$$(\ell-1) \, a^{\mathrm{D}}_{\ell-1,0} = \varepsilon_0 \, R^{\ell+1} \, \Omega \, \sqrt{(\ell-1) \, (\ell+1)} \, J_{\ell,0} \, f^{\mathrm{B}}_{\ell,0}(R).$$

$\Rightarrow$ constants of integration fully determined by $f^{\mathrm{B}}_{\ell,m}(R)$.

Any exact analytical vacuum solution requires only knowledge about $B^r(R)$.

Typical magnetic topology

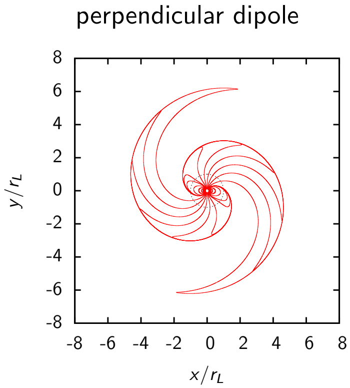

$(\ell, m) = (1, 1)$

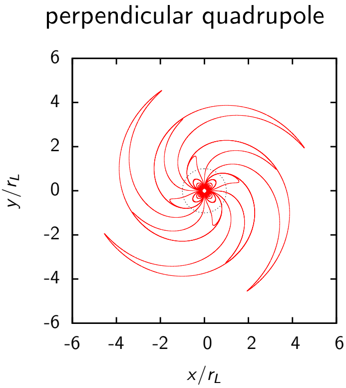

$(\ell, m) = (2, 2)$

Some observables related to multipolar emission

For any magnetic multipole of order ℓ, useful observables are

- the spindown luminosity

$$L \propto B^2 \, \Omega^{2\,\ell+2} \, R^{2\,\ell+4}$$

- the braking index. Efficiency of braking given by the braking index n such that

$$\dot{\Omega} = -K \, \Omega^n$$

$\Rightarrow$ For a multipole of order ℓ it becomes approximately

$$n = 2\,\ell + 1$$

- for a dipole $n = 3$.
- for a quadrupole $n = 5$ (the same for gravitational radiation).

Braking index: observations

Pulsar	Distance (kpc)	Period P (s)	$\dot{P}$ (10^{-15})	Braking de index n	References
B0531+21	2.0	0.033	421	2.509 ± 0.001	Lyne et al. (1993)
J0537-6910	51	0.0161	0.0518	-1.5 ± 0.1	Middleditch et al. (2006
B0540-693	51.5	0.050	479	2.140 ± 0.009	Livingstone et al. (2005
B0833-45	0.29	0.089	124	1.40 ± 0.20	Lyne et al. (1996)
B1509-58	5.81	0.150	1490	2.837 ± 0.001	Kaspi et al. (1994)
J1846-0258	5.10	0.325	7083	2.65 ± 0.01	Livingstone et al. (2006
				2.16 ± 0.13	Livingstone et al. (2011
J1119-6127	8.40	0.408	4021	2.91 ± 0.05	Weltevrede et al. (2011)
J1734-3333		1.170	2280	0.9 ± 0.2	Espinoza et al. (2011)
J1833-1034				1.857	Roy et al. (2012)
J1640-4631	12	0.206	975.8	3.15	Archibald et al. (2016)

Table: Observational properties of some typical pulsars.

1. A simple question

2. Exact solutions
   - General outgoing wave solution
   - Single multipole solution
   - Off-centered dipole
   - Radiating off-centred dipole

3. Results
   - Field line topology
   - Spindown luminosity
   - Implications for pulsed emission
   - Polarisation

4. Conclusions & Perspectives

Magnetic field topology

Why study more general magnetic field configurations?

- centered dipole is a simple prescription for stellar magnetic field but probably to simplistic for real applications.
- off-centered dipole and multipoles useful for main sequence stars (to explain polarisation profile among others).

Two important vectors for the geometry of an off-centred dipole

- magnetic dipole moment $\mathbf{m}$.
- displacement vector $\mathbf{d}$ w.r.t the stellar centre.

leading to a static magnetic field

$$\mathbf{B} = \frac{B\,R^3}{\|\mathbf{r}-\mathbf{d}\|^3}\left[\frac{3\,\mathbf{m}\cdot(\mathbf{r}-\mathbf{d})}{\|\mathbf{r}-\mathbf{d}\|^2}\,(\mathbf{r}-\mathbf{d})-\mathbf{m}\right]$$

Geometry of the decentred dipole

Most general configuration given by

- (α, β) magnetic moment μ orientation.
- (d, δ) displacement vector d in xOz plane.
- obviously $d < R$!!!
- two additional parameters related to observations
  - the line of sight inclination ζ.
  - emission height h.

Idea: expansion of an off-centred dipole in terms of a (infinite) series of centred multipoles.

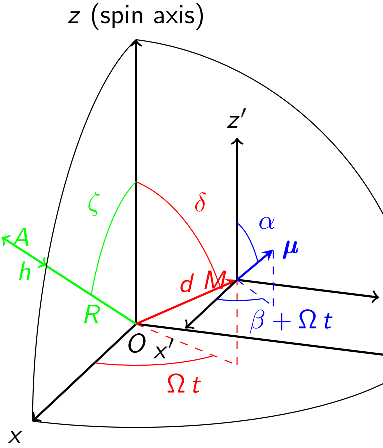

Figure: Geometry of the decentred dipole: important angles $\{\alpha, \beta, \delta\}$ and the distance d.

Radial magnetic field series expansion to quadrupole order

The first expansion coefficients including the dipole and quadrupole are given by

$$f_{1,0}^{\mathrm{B}} = -\sqrt{\frac{8\,\pi}{3}}\,\frac{B\,R^3}{r^2}\,\cos\alpha$$

$$f_{1,1}^{\mathrm{B}} = \sqrt{\frac{16\,\pi}{3}}\,\frac{B\,R^3}{r^2}\,\sin\alpha\,e^{-i\,\beta}$$

$$f_{2,0}^{\mathrm{B}} = -\sqrt{\frac{6\,\pi}{5}}\,\frac{B\,R^3}{r^2}\,\epsilon\,(2\,\cos\alpha\,\cos\delta - \sin\alpha\,\sin\delta\,\cos\beta)$$

$$f_{2,1}^{\mathrm{B}} = 6\,\sqrt{\frac{\pi}{5}}\,\frac{B\,R^3}{r^2}\,\epsilon\,(\cos\alpha\,\sin\delta + \sin\alpha\,\cos\delta\,e^{-i\,\beta})$$

$$f_{2,2}^{\mathrm{B}} = -6\,\sqrt{\frac{\pi}{5}}\,\frac{B\,R^3}{r^2}\,\epsilon\,\sin\alpha\,\sin\delta\,e^{-i\,\beta}$$

Expansion in ϵ^k ($\epsilon = d/R$), k related to multipolar components $k = \ell - 1$.

- ϵ^0: pure dipole (the well known centred one).
- ϵ^1: quadrupole corrections.
- ϵ^2: hexapole corrections, and so on ...

The off-centred dipole expansion

Including only the first order corrections in ϵ that is quadrupolar corrections

$$\mathbf{F}^{\rm off} = \mathbf{F}^{\rm dip}(\psi \to \psi - \beta) + \epsilon \left[(2 \cos\alpha \cos\delta - \sin\alpha \sin\delta \cos\beta) \, \mathbf{F}^{\rm quad}_{m=0}(\psi) + \cos\alpha \sin\delta \, \mathbf{F}^{\rm quad}_{m=1}(\psi) + \sin\alpha \cos\delta \, \mathbf{F}^{\rm quad}_{m=1}(\psi \to \psi - \beta) + \sin\alpha \sin\delta \, \mathbf{F}^{\rm quad}_{m=2}(2\,\psi \to 2\,\psi - \beta) \right] + \epsilon^2 \, (\text{higher order multipoles } \ell > 2)$$

F is any vector of the electromagnetic field $(\mathbf{D}, \mathbf{B})$.

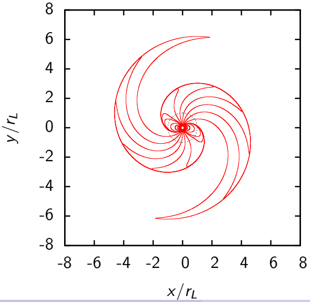

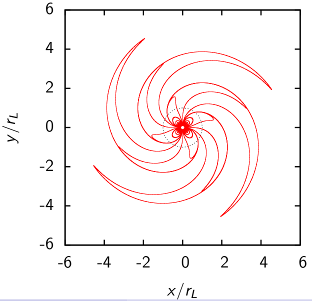

1. A simple question

2. Exact solutions
   - General outgoing wave solution
   - Single multipole solution
   - Off-centered dipole
   - Radiating off-centred dipole

3. Results
   - Field line topology
   - Spindown luminosity
   - Implications for pulsed emission
   - Polarisation

4. Conclusions & Perspectives

Orthogonal case 1

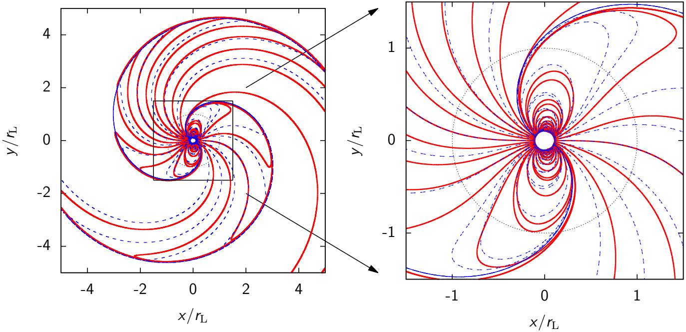

Figure: A sample of magnetic field lines for the offset perpendicular dipole with $a = R/r_L = 0.1$ and $\epsilon = 0.2$ are shown in red solid line for $\beta = 0^\circ$. The centred perpendicular dipole is shown in blue dashed line.

Orthogonal case 2

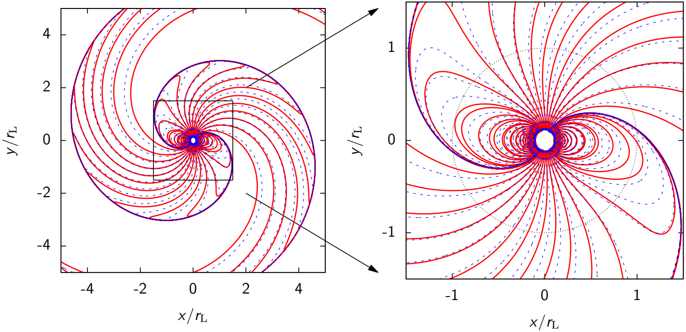

Figure: A sample of magnetic field lines for the offset perpendicular dipole with $a = 0.1$ and $\epsilon = 0.2$ are shown in red solid line for $\beta = 90^\circ$. The centred perpendicular dipole is shown in blue dashed line.

Spindown and recoil

For the dipole and quadrupole contributions

$$L_{m=1} = L_{\rm dip} \left[\left(1 - a^2\right) \sin^2\alpha + \frac{24}{25} \, a^2 \, \epsilon^2 \, \cos^2\alpha \right]$$

$$L_{m=2} = \frac{48}{5} \, L_{\rm dip} \, a^2 \, \epsilon^2 \, \sin^2\alpha$$

- typical $(1 - a^2) \sin^2\alpha$ dependence of the luminosity for a centred finite size dipole when $\epsilon = 0$.
- as for the point dipole, corrections of second order in a and ϵ, in the form $a^2 \, \epsilon^2$.
- some corrections added with respect to (Harrison & Tademaru, 1975).

The electromagnetic recoil is given by

$$F_{m=1} = \frac{6}{5} \, \frac{L_{\rm dip}}{c} \, a \, \epsilon \, \cos\alpha \, \sin\alpha \, \sin\beta$$

$$F_{m=2} = \frac{256}{105} \, \frac{L_{\rm dip}}{c} \, a^3 \, \epsilon^3 \, \cos\alpha \, \sin\alpha \, \sin\beta.$$

The emission sites

Three important emission regions

- polar cap.
- outer gap/slot gap.
- striped wind.

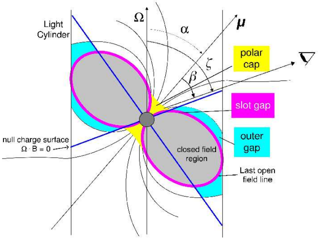

All three show possible phase lag between centred and off-centered dipoles.

see next talk by Anu Kundu.

(Pétri, 2016)

1. A simple question
2. Exact solutions
   - General outgoing wave solution
   - Single multipole solution
   - Off-centered dipole
   - Radiating off-centred dipole
3. Results
   - Field line topology
   - Spindown luminosity
   - Implications for pulsed emission
   - Polarisation
4. Conclusions & Perspectives

Extension of the rotating vector model

Polarisation angle is given by

$$\tan\psi = \frac{(\boldsymbol{\Omega} \wedge \mathbf{n}_{\rm p}) \cdot \mathbf{n}_{\rm obs}}{\boldsymbol{\Omega} \cdot \mathbf{n}_{\rm p}}.$$

where

$$(\boldsymbol{\Omega} \wedge \mathbf{n}_{\rm p}) \cdot \mathbf{n}_{\rm obs} = (1 + \eta - \epsilon \cos\delta \cos\zeta) \sin\alpha \sin(\beta + \varphi)$$
$$+ \epsilon \sin\delta (\cos\alpha \cos\zeta \sin\varphi - \sin\alpha \sin\beta \sin\zeta)$$
$$\boldsymbol{\Omega} \cdot \mathbf{n}_{\rm p} = (1 + \eta) (\cos\alpha \sin\zeta - \sin\alpha \cos\zeta \cos(\beta + \varphi))$$
$$+ \epsilon (\sin\alpha \cos\delta \cos(\beta + \varphi) - \cos\alpha \sin\delta \cos\varphi).$$

- $\Rightarrow$ for $\epsilon = 0$ it reduces to the RVM.
- $\Rightarrow$ altitude dependent polarisation through η.

(Pétri, 2017)

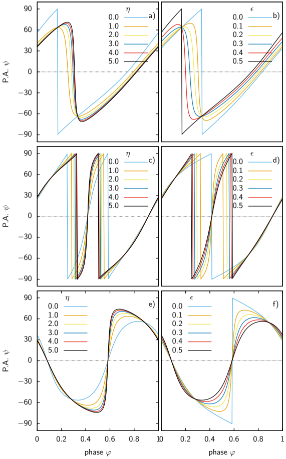

Conclusions & Perspectives

Achievements

- multipoles naturally arise in an off-centred rotating dipole.
- strength of multipoles set completely by geometry.
- multipoles decaying like $1/r$ as for the dipole.
- possible signature in the wave (striped wind) zone as time lag.
- clear signature expected in the polarisation profile.

Perspectives

- detailed analysis of consequences on electrodynamics and emission properties.
- what about FFE decentred magnetospheres?
- re-explore time lag between radio and gamma-ray pulses ($\delta - \Delta$ relation).

References I

Archibald R. F. et al., 2016, ApJ, 819, L16

Deutsch A. J., 1955, Annales d'Astrophysique, 18, 1

Espinoza C. M., Lyne A. G., Kramer M., Manchester R. N., Kaspi V. M., 2011, ApJ, 741, L13

Harrison E. R., Tademaru E., 1975, \apj, 201, 447

Kaspi V. M., Manchester R. N., Siegman B., Johnston S., Lyne A. G., 1994, ApJ, 422, L83

Livingstone M. A., Kaspi V. M., Gavriil F. P., 2005, ApJ, 633, 1095

Livingstone M. A., Kaspi V. M., Gotthelf E. V., Kuiper L., 2006, ApJ, 647, 1286

Livingstone M. A., Ng C.-Y., Kaspi V. M., Gavriil F. P., Gotthelf E. V., 2011, ApJ, 730, 66

Lyne A. G., Pritchard R. S., Graham-Smith F., 1993, MNRAS, 265, 1003

Lyne A. G., Pritchard R. S., Graham-Smith F., Camilo F., 1996, Nature, 381, 497

Middleditch J., Marshall F. E., Wang Q. D., Gotthelf E. V., Zhang W., 2006, ApJ, 652, 1531

Pétri J., 2015, Monthly Notices of the Royal Astronomical Society, 450, 714

References II

Pétri J., 2016, Monthly Notices of the Royal Astronomical Society, 463, 1240

Pétri J., 2017, Monthly Notices of the Royal Astronomical Society: Letters, 466, L73

Radhakrishnan V., Cooke D. J., 1969, \aplett, 3, 225

Roy J., Gupta Y., Lewandowski W., 2012, MNRAS, 424, 2213

Weltevrede P., Johnston S., Espinoza C. M., 2011, MNRAS, 411, 1917

Magnetic field strength estimates

- luminosity L, stellar radius R and period P (or Ω) being known, we cant get an estimate of the magnetic field strength at the surface.
- usually done for a pure dipole.
- but if multipoles are present, the estimate becomes inaccurate or even wrong.

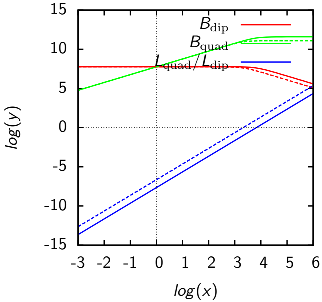

Normal pulsar $L_{\rm dip} \gg L_{\rm quad}$

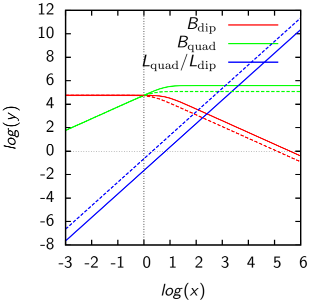

Millisecond pulsar

Magneto-dipole losses useless to get drastic upper limits for multipole components.

$$L_{\rm dip} \gg L_{\rm quad} \not\Leftrightarrow B_{\rm dip} \gg B_{\rm quad}$$

Time lag due to off-centered dipole

Current sheet in striped wind as two-armed spiral in equatorial plane such that

$$\varphi = \Omega\, t - k\,(r - R) + \psi(r, a, \epsilon) + \varphi_0$$

Several special cases of interest for emission sites

- at the surface, $\psi_* = \psi(R, a, \epsilon)$: polar cap.
- at the light cylinder $\psi_{\rm L} = \psi(r_{\rm L}, a, \epsilon)$: outer gap.
- at infinity $\psi_\infty = \psi(\infty, a, \epsilon)$: striped wind.

In general there is an imprint of multipolar fields also in the wave zone.
For flow with speed V, discrepancy to perfect archimedean spiral contained in ψ such that

$$\varphi = \Omega\,\left(t - \frac{r - R}{V}\right) + \psi(r, a, \epsilon) + \varphi_0.$$

The time lag induced by the shifted spiral is

$$\frac{\Delta t^r}{P} \approx \frac{1}{2\,\pi}\,\left[\frac{r_2 - r_1}{2\,\Gamma^2\,r_{\rm L}} + \psi_1 - \psi_2\right].$$

where 1 and 2 are your favorite emission sites for radio and/or high energy photons.

Comparison between vacuum, split monopole and FFE

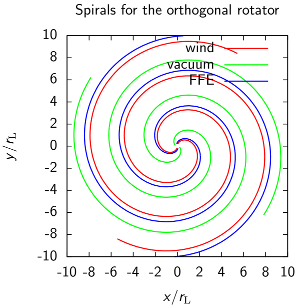

Figure: Location of the spiral structure for the striped wind (red), the vacuum (green) and the force-free (blue) solution for the orthogonal rotator.

Braking index: theory

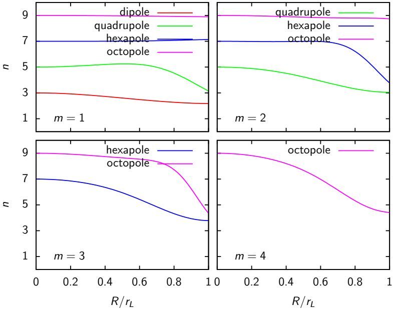

Figure: Braking index of rotating magnetic multipoles.

$$a = \frac{R}{r_{\mathrm{L}}} = \frac{\Omega\, R}{c} \propto \Omega \propto 1/P$$

- $1 < n < 3 \Rightarrow$ topology between monopolar wind and dipolar radiation.
- $3 < n < 5 \Rightarrow$ topology between dipolar and quadrupolar radiation.